RESEARCH ACTIVITIES III
Department of Electronic Structure

III-A Synthesis and Characterization of Exotic Molecule Based Nano-Crystals of Metal Acetylides: Toward Carbon Encapsulated Metal Dot Array, Metal Nano-Networks and Metal-Carbon Hybrid Systems

Metal-carbon binary junctions are expected to exhibit interesting properties, such as Shottoky barrier rectification, optical and tunneling devices, and chemical protector against oxidation. Metal acetylides have the ionic bond between the metallic cation and the acetylide anion. In the simplest case, divalent metal cations (M^{2+}) form a fcc lattice structure with a C_2^{2-} anion between the two metal cations. The introduction of alkyl or aromatic group into the C_2 unit, producing $R–C{\equiv}C^-$, can generate organometallic cluster compounds $((R–C{\equiv}C^-)_aM^{a+})_n$, ($a$ = 1, 2), some of which can be isolated as single crystals. These cluster compounds are soluble in organic solvent and provide solid films with nano-scale planarity by spin-coating method. Photoexcitation of metal-acetylides induces charge-neutralization reaction producing carbon-skinned metal particles, metallic nanowires or nano-sheets covered with organic polymer matrices. This property leads us to apply for photo-lithographical pattern generation of metallic circuits or magnetic arrays. On the other hand, the reaction mechanism of the photoreactions of the respective acetylide systems can be highly dependent on the electronic structure of metal atoms. We are also illuminating the mechanism of these reactions.

III-A-1 Self-Assembled Nanowire Synthesis of Highly-Anisotropic Copper Acetylide Molecules

JUDAI, Ken; NISHIJO, Junichi; OKABE, Chie; NISHI, Nobuyuki

Various methods have been suggested for metallic and semiconductive nanowire production, template based synthesis, vapor-liquid-solid growth, solution-liquid-solid process, oxide-assisted growth and so on. Above all, the production using a highly anisotropic crystal can be regarded as due to self-assembly of small molecules or atoms to a nanowire. The self-assembly method has potential advantage of relatively low cost, high purity, and large-scale production. However, only limited materials have anisotropic properties, for example, molybdenum chalcogenides, selenium, and tellurium. Besides, it is very hard to produce thin nanowires by only highly anisotropic properties. Here we report a new compound having a highly anisotropic crystal structure. Copper acetylide (C_2Cu_2) molecules self-assemble into ultra thin nanowires under an extremely slow nucleation condition. Moreover, annealing of the C_2Cu_2 nanowires converts to copper nanocables encapsulated in carbon outer layers. The copper nanocable core is extremely thin, in which only 8 Cu atoms can line up in the diameter.

One of the merits of self-assembly nanowire production is an extremely simple procedure of just preparing only a building block. The C_2Cu_2 nanowire can be also generated facilely. Figure 1 shows a scanning electron microscopy (SEM) image of C_2Cu_2 products on silicon substrates, where the C_2Cu_2 suspension in methanol has been dropped onto and air-dried. Nanowire morphology was observed when the C_2H_2 exposing rate was kept extremely slow (0.05 mL/min). Although C_2Cu_2 was synthesized by chemical reaction of gram-order production in a flask, microscopic shape of the product is a nanoscale needle-like crystal. This indicates that C_2Cu_2 molecules aggregate and self-assemble into nanowire morphology in an aqueous solution. On the contrary to the successful production of nanowires, a fast exposing rate of C_2H_2 gas gave amorphous products. The key step of self-assembling for the nano-structure is just only the control of the nucleation rate of acetylide molecules.

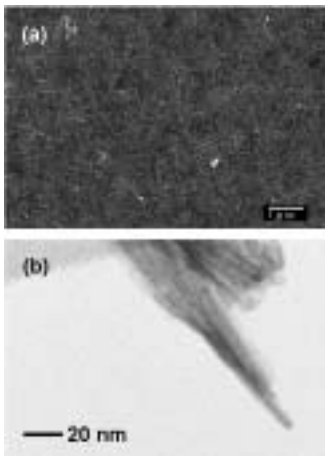

Figure 1. (a) SEM image of C_2Cu_2 precipitate. Nanowire morphology can be obtained in the extremely slow nucleation condition. (b) TEM image of an end of a budle of C_2Cu_2 wires.

III-A-2 Photochemical Conversion of (Cu^+ $C{\equiv}C^-$-*t*-Butyl)$_{24}$ Cluster Molecules to Cu Metallic Nano-Sheets Embedded in Polymer Nano-Film

NISHI, Nobuyuki; NISHIJO, Junichi; OKABE, Chie; OISHI, Osamu; JUDAI, Ken

Only a limited number of the cluster molecules with more than 20 metal atoms is known as structure-analyzed clusters. Olblich *et al.* reported the synthetic method and X-ray diffraction analysis of (Cu^+ $C{\equiv}C^-$-*t*-Butyl)$_{24}$ in1993. This molecule is soluble and show red emission in *n*-hexane but its electronic absorption spectrum exhibits concentration dependence originated from molecular association. The association occurs in the concentration higher than 1×10^{-4} M. The spectral pattern of the thin film of this molecule is essentially the same as that of 1×10^{-3} M solution of *n*-hexane, showing a peak at 228 nm and a shoulder at 282 nm The absorption threshold is seen at 510 nm. This absorption feature is essentially the same as those of monomer or dimer species of similar complex molecules. Cluster formation changes little of the electronic structure indicating very weak metal-metal interactions in these multinuclear cluster molecules. From the analogy of similar systems of various coordinated copper clusters, the emission is believed to originate from the triplet metal-ethynyl charge transfer state rather localized in a single pair. No emission is seen from the thin films and one can expect the presence of radiationless pathways for heat generation or reaction channel(s). The UV absorption spectrum of the spin-coated film shows a peak at 232 nm and a shoulder 282 nm that is accompanied with the tail at 400 nm to 520 nm and the broad absorption (or background) down to near infrared region. The last broad extension is believed due to the optical scattering characteristics of the thin film. Thus, the photoexcitation of the film is expected to cause energy transfer in the triplet state. This molecule has 24 Cu-ethynyl groups and intracluster T-T annihilation can be induced. The infrared spectrum of the film also changes upon photoexcitation. The original cluster shows a doublet band at 1455 and 1474 cm^{-1} characteristic of the coupled two -C≡C$^-$ bonds. On the photo-illumination, new bands appear at higher frequencies, 1552 and 1573 cm^{-1}. This indicates that the charge neutralization produces strong double bond networks around metallic copper fragments. Figure 1 shows the Transmission Electron Microscope (TEM) images of the film heated at 250 °C (left) and that irradiated with UV light from a 500W high pressure mercury lamp. The heating produces Cu nanoparticles with spherical or polyhedral shapes. The dominant sizes of the particles are 3.3 nm, 5.2 nm, 7 nm, 10.5 nm and 14 nm, suggesting the growth due to particle joining. On the other hand, photoexcitation causes growth of cubic crystals or planer copper sheets joining together and extending the metallic area wider and wider. Since the photoexcitation puts the energy into the metal atoms rather predominantly, the neutralized metal atoms are thought to cohere in the original crystal planes where the Cu cations are located. The heating may excites both metal atoms and organic parts simultaneously and allow the metal atoms cohere three dimentionally.

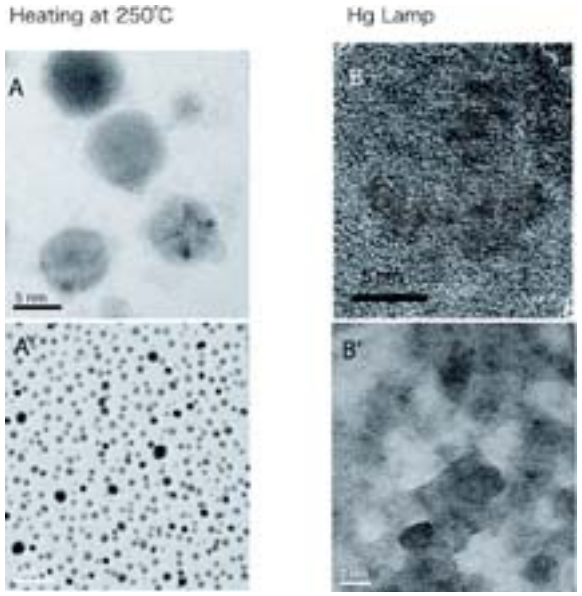

Figure 1. High resolution TEM images of heated (left; A and A') and photoexcited (right; B and B') (Cu^+ $C{\equiv}C^-$-*t*-Butyl)$_{24}$ cluster films on collodion membranes.

III-A-3 Guest Controlled Magnetism of CoC_2 Nanoparticles

NISHIJO, Junichi; JUDAI, Ken; NISHI, Nobuyuki

The structure of molecule-based magnets is often affected by gas or solvent absorption owing to their flexibility, and the flexibility opens up the way for controlling their magnetism by a chemical environment. We discovered that the molecule-based magnet CoC_2 is an outstanding example of the "controllable magnet."

The as-prepared anhydrous CoC_2 shows superparamagnetic behavior down to 2.5 K with the Curie constant of C = 2.5 emu K/mol and saturation magnetization of M_S = 1.5 μ_B. Below 2.5 K, a small part of anhydrous CoC_2 shows ferromagnetic (FM) behavior, but the major part of anhydrous CoC_2 are still superparamagnetic. The large Curie constant indicates the short range strong FM interaction between Co^{2+} cations. Though the existence of strong FM interactions, orientation disorder of the C_2^{2-} brings the weakening of the interaction in many places and prevents the FM transition. Once the material is exposed to ammonia gas, the CoC_2 absorbs ammonia molecules accompanied by orientation ordering of the C_2^{2-}. The orientation ordering also means that the strength of the interaction between spins tend to be uniform. Indeed, the increase in the Curie constant from 2.5 to 3.5 emu K/mol by ammonia absorption suggests that the area of short range FM ordering is expanded by absorption, while the M_S keeps same value. The absorbed ammonia molecules are easily desorbed under ammonia-free condition. The desorption lowers the Curie constant from 3.5 to 2.7 emu K/mol. The decrease of the Curie constant is explained by the partial orientation disorder of C_2^{2-}; that

is, desorption process disturbs the orientation of C_2^{2-} again, which reduces the range of the FM short range ordering. After the 1st absorption/desorption cycle, the Curie constant changes reversibly from 3.2 to 2.7 emu K/mol for ammonia absorbed and desorbed CoC_2, respectively.

The field-cooled (FC, 10 Oe) and zero field-cooled (ZFC) susceptibilities for ammonia absorbed and desorbed CoC_2 are shown in figure 1. The 1st absorption raises both FC susceptibility and blocking temperature of T_B = 20 K, which is indicated by the peak of ZFC susceptibility. Desorption lowers ZFC susceptibility and T_B, but the values are still larger than those of anhydrous CoC_2. After the 1st absorption/desorption cycle, though the ZFC susceptibility and T_B of ammonia absorbed CoC_2 is little smaller than that of 1st cycle, the magnetism changes reversibly by absorption and desorption of ammonia. The T_B and the ZFC susceptibility at 1.8 K are raised from 5 K and 7.5 emu/mol to 10 K and 17 emu/mol, respectively, by ammonia absorption.

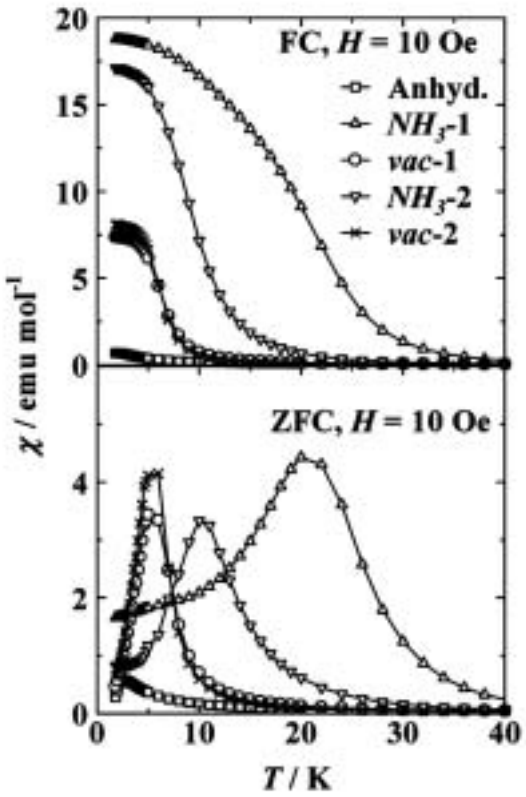

Figure 1. Field-cooled (FC) and zero field-cooled (ZFC) susceptibilities of ammonia absorbed/desorbed CoC_2. The legends *NH_3*-i and *vac*-i indicate the i-th times ammonia.

III-A-4 Formation of Carbon-Encapsulated Metallic Nano-Particles from Metal Acetylides by Electron Beam Irradiation

NISHIJO, Junichi; OKABE, Chie; BUSHIRI, Junaid M.; KOSUGI, Kentaroh; NISHI, Nobuyuki; SAWA, Hiroshi

[*Eur. Phys. J. D* **34**, 219–222 (2005)]

Transition metal acetylides, MC_2 (M = Fe, Co and Ni), exhibit ferromagnetic behavior of which T_C is characteristic of their size and structure. CoC_2 synthesized in anhydrous condition exhibited cubic structure with disordered C_2^{2-} orientation. Once being exposed to water (or air), the particles behave ferromagnetically due to the lengthening of the Co–Co distance by the coordination of water molecules to Co^{2+} cations. Heating of these particles induces segregation of metallic cores with carbon mantles. Electron beam or 193 nm laser beam can produce nanoparticles with metallic cores covered with carbon mantles.

III-A-5 Reexamination of the Structures and Energies of Li_2C_2 and Li_4C_4

LEE, Sang-Yeon[1]; BOO, Bong-Hyun[2]; KANG, Heun-Kag[2]; KANG, Dongeun[2]; JUDAI, Ken; NISHIJO, Junichi; NISHI, Nobuyuki
([1]Kyungpook Natl. Univ.; [2]Chungnam Natl. Univ.)

[*Chem. Phys. Lett.* **411**, 484–491 (2005)]

The structures and energies of Li_2C_2 and Li_4C_4 have been reexamined by DFT and MP2 methods using a variety of basis sets of 6-311+G(3df) and cc-pVXZ(X = T,Q,5). Two low-lying isomers are found as the local minima on the potential energy surfaces of Li_4C_4. The lowest energy structure is shown to be multiply bridged D_{2h} form. A newly found quadruply bridged C_i form is found to be a local minimum, lying in energy above D_{2h} form by 22 kJ/mol in the energy. Also the energetics of high-lying isomers such as tetralithiotetrahedrane isomers were evaluated and discussed.

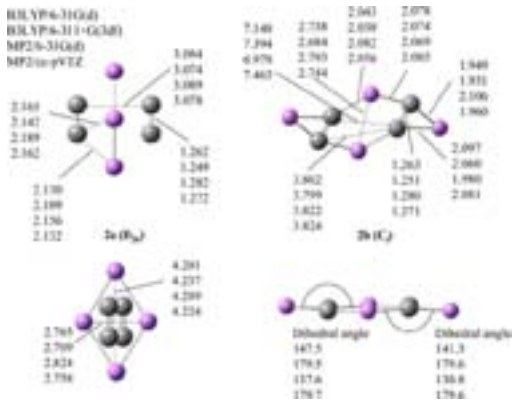

Figure 1. Geometries of low-lying isomers of Li_4C_4 optimized by the various methods indicated herein.

III-B Ultrafast Dynamics and Scanning Tunneling Microscopy

Proton transfer and geometrical isomerization processes in electronic excited states are investigated with our pico-femto dual wavelength valuable systems. For the study of molecules on metallic or crystalline surface, very low temperature Scanning Tunneling Microscope (LT STM) system are now in use for collaboration with users in universities.

III-B-1 Excited-State Double-Proton Transfer in the 7-Azaindole Dimer in Gas Phase 3. Reaction Mechanism Studied by Picosecond Time-Resolved REMPI Spectroscopy

SAKOTA, Kenji[1]; OKABE, Chie; NISHI, Nobuyuki; SEKIYA, Hiroshi[1]
([1]Kyushu Univ.)

[*J. Phys. Chem. A* **109**, 5245–5247 (2005)]

The excited state double-proton transfer (ESDPT) reaction in the jet-cooled 7-azaindole dimer ($7AI_2$) has been investigated with the picosecond time-resolved resonance-enhanced multiphoton ionization spectroscopy. The observed decay profiles of $7AI_2$ by exciting the origin and the intermolecular stretch fundamental in the S_1 state are well reproduced by single exponential functions with time constants of 1.9±0.9 ps and 860± 300 fs, respectively. This result provides a clear evidence of the concerted mechanism of ESDPT in $7AI_2$.

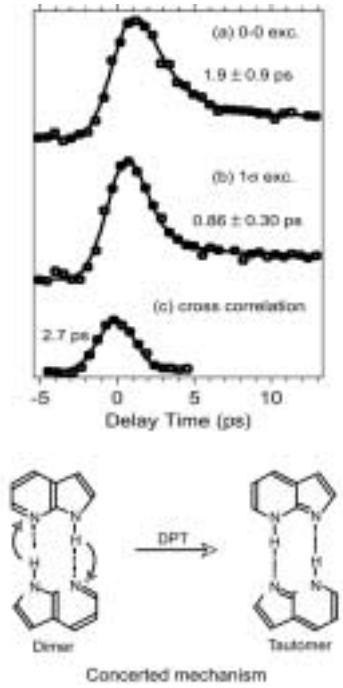

Figure 1. Top: Decay profiles of $7AI_2$ pumped at (a) the origin and (b) the intermolecular stretching band, respectively. The wavelength of the probe laser was fixed at 620 nm in (a) and (b). The open circles are experimental data, while the solid curves are best-fitted curves obtained by biexponential functions. The cross correlation trace is also indicated in (c). The instrumental time resolution given by the fwhm of the cross-correlation trace is 2.7 ps.
Bottom: Scheme of concerted mechanism.

III-B-2 Ultrafast Excited-State Dynamics in Photochromic *N*-Salicylideneaniline Studied by Femtosecond Time-Resolved REMPI Spectroscopy

OKABE, Chie; NAKABAYASHI, Takakazu[1]; INOKUCHI, Yoshiya; NISHI, Nobuyuki; SEKIYA, Hiroshi[2]
([1]Hokkaido Univ.; [2]Kyushu Univ.)

[*J. Chem. Phys.* **121**, 9436–9422 (2004)]

Ultrafast processes in photoexcited *N*-salicylideneaniline have been investigated with femtosecond time-resolved resonance-enhanced multiphoton ionization spectroscopy. The ion signals *via* the $S_1(n,\pi^*)$ state of the enol form as well as the proton-transferred *cis*-keto form emerge within a few hundred femtoseconds after photoexcitation to the first $S_1(\pi,\pi^*)$ state of the enol form. This reveals that two ultrafast processes, excited-state intramolecular proton transfer (ESIPT) reaction and an internal conversion (IC) to the $S_1(n,\pi^*)$ state, occur on a time scale less than a few hundred femtoseconds from the $S_1(\pi,\pi^*)$ state of the enol form. The rise time of the transient corresponding to the production of the proton-transferred *cis*-keto form is within 750 fs when near the red edge of the absorption is excited, indicating that the ESIPT reaction occurs within 750 fs. The decay time of the $S_1(\pi,\pi^*)$ state of the *cis*-keto form is 8.9 ps by exciting the enol form at 370 nm, but it dramatically decreases to be 1.5–1.6 ps for the excitation at 365–320 nm. The decrease in the decay time has been attributed to the opening of an efficient nonradiative channel; an IC from $S_1(\pi,\pi^*)$ to $S_1(n,\pi^*)$ of the *cis*-keto form promotes the production of the *trans*-keto form as the final photochromic products. The two IC processes may provide opposite effect on the quantum yield of photochromic products: IC in the enol form may substantially reduce the quantum yield, but IC in the *cis*-keto form increase it.

III-B-3 Orientation of Nitrous Oxide on Palladium(1 1 0) by STM

WATANABE, Kazuo[1]; KOKALJ, Anton[2]; INOKUCHI, Yoshiya[1]; RZEZNICKA, Izabela[3]; OHSHIMO, Keijiro; NISHI, Nobuyuki; MATSUSHIMA, Tatsuo[3]
([1]Univ. Tokyo; [2]J. Stefan Inst.; [3]Hokkaido Univ.)

[*Chem. Phys. Lett.* **406**, 474–478 (2005)]

The adsorption structure of N_2O on Pd(110) was analyzed below 14 K by scanning-tunneling microscopy. The N_2O monomer was oriented along the [001]

direction in the on-top form. Furthermore, the formation of small aggregates extending along the direction was observed. The observed images were well-simulated for two types of cluster structures optimized by density-functional theory calculations. The components in the aggregates are proposed to be in a tilted form either on bridge sites or on-top sites.

III-C Spectroscopic and Dynamical Studies of Molecular Cluster Ions

Electron defficiency of molecular cluster cations can attract electron rich groups or atoms exhibiting charge transfer or charge resonance interaction in the clusters. This causes dynamical structural change such as proton transfer or ion-core switching in hot cluster ions or clusters in solution.

III-C-1 Infrared Photodissociation Spectra and Solvation Structure of $Mg^+(CH_3OH)_n$ (n = 1–4)

MACHINAGA, Hironobu[1]; OHASHI, Kazuhiko[1]; INOKUCHI, Yoshiya[2]; NISHI, Nobuyuki; SEKIYA, Hiroshi[1]
([1]Kyushu Univ.; [2]Univ. Tokyo)

[*Chem. Phys. Lett.* **391**, 85–90 (2004)]

The infrared photodissociation spectra of mass-selected $Mg^+(CH_3OH)_n$ (n = 1–4) are measured and analyzed with the aid of density functional theory calculations. Hydrogen bonding between methanol molecules is found to be absent in $Mg^+(CH_3OH)_3$, but detected in $Mg^+(CH_3OH)_4$ through characteristic frequency shifts of the OH stretch of methanol. The maximum number of the methanol molecules that can be directly bonded to the Mg^+ ion is limited to three and the fourth molecule starts to fill the second solvation shell. The vibrational spectroscopy provides clear evidence for the closure of the first shell at n = 3.

III-C-2 Infrared Photodissociation Spectroscopy of $Mg^+(NH_3)_n$ (n = 3–6): Direct Coordination or Solvation through Hydrogen Bonding

OHASHI, Kazuhiko[1]; TERABARU, Kazutaka[1]; INOKUCHI, Yoshiya[2]; MUNE, Yutaka[1]; MACHINAGA, Hironobu[1]; NISHI, Nobuyuki; SEKIYA, Hiroshi[1]
([1]Kyushu Univ.; [2]Univ. Tokyo)

[*Chem. Phys. Lett.* **393**, 264–270 (2004)]

The infrared photodissociation spectra of mass-selected $Mg^+(NH_3)_n$ (n = 3–6) are measured and analyzed with the aid of density functional theory calculations. No large frequency reduction is observed for the NH stretches of ammonia, suggesting that either all the ammonia molecules coordinate directly to the Mg^+ ion or an additional ammonia in the second shell bridges two ammonias in the first shell through hydrogen bonds. Four or possibly five ammonia molecules are allowed to occupy the first shell, in striking contrast to the closure of the first shell in $Mg^+(H_2O)_3$.

III-C-3 Electronic Spectra of Jet-Cooled 3-Methyl-7-Azaindole Dimer. Symmetry of the Lowest Excited Electronic State and Double-Proton Transfer

HARA, Akihiko[1]; KOMOTO, Yusuke[1]; SAKOTA, Kenji[1]; MIYOSHI, Riko[1]; INOKUCHI, Yoshiya; OHASHI, Kazuhiko[1]; KUBO, Kanji[1]; YAMAMOTO, Emi[1]; MORI, Akira[1]; NISHI, Nobuyuki; SEKIYA, Hiroshi[1]
([1]Kyushu Univ.)

[*J. Phys. Chem. A* **108**, 10789–10793 (2004)]

The fluorescence excitation spectra are recorded for jet-cooled dual hydrogen-bonded 3-methyl-7-azaindole dimer $(3MAI)_2$-*hh* and deuterated dimers $(3MAI)_2$-*hd* and $(3MAI)_2$-*dd* near the electronic origin region of the S_1–S_0 transition, where *hd* and *dd* indicate the deuteration of an imino hydrogen and two imino hydrogens, respectively. A single origin is detected in the spectra of $(3MAI)_2$-*hh* and $(3MAI)_2$-*dd*, whereas two electronic origins separated by 13 cm^{-1} are detected in the spectrum of $(3MAI)_2$-*hd*. The excited-state double-proton transfer (ESDPT) occurs in $(3MAI)_2$-*hh*, while $(3MAI)_2$-*hd* and $(3MAI)_2$-*dd* undergo excited-state proton/deuteron transfer and excited-state double deuteron transfer, respectively. In $(3MAI)_2$-*hd*, the excitation is localized on either the 3MAI-*h* or 3MAI-*d* moiety. The localization of the excitation is explained by a weak coupling of the excitonic states of $(3MAI)_2$-*hh* and $(3MAI)_2$-*dd*. The effective symmetry of the lowest excited state of $(3MAI)_2$-*hh* and $(3MAI)_2$-*dd* belongs to the C_{2h} point group, while that of $(3MAI)_2$-*hd* belongs to the C_s point group. The vibronic patterns in the excitation spectra of the $(3MAI)_2$ dimers is very similar to those of the 7-azaindole dimers, indicating that the methyl substitution provides little effect on the shape of the ESDPT potential.

III-C-4 Structures of $[(CO_2)_n(H_2O)_m]^-$ (n = 1–4, m = 1, 2) Cluster Anions. I. Infrared Photodissociation Spectroscopy

MURAOKA, Azusa[1]; INOKUCHI, Yoshiya[1]; NISHI, Nobuyuki; NAGATA, Takashi[1]
([1]Univ. Tokyo)

[*J. Chem. Phys.* **122**, 094303 (7 pages) (2004)]

The infrared photodissociation spectra of $[(CO_2)_n(H_2O)_m]^-$ (n = 1–4, m = 1, 2) are measured in the 3000–3800 cm^{-1} range. The $[(CO_2)_n(H_2O)_1]^-$ spectra are characterized by a sharp band around 3570 cm^{-1} except for n = 1; $[(CO_2)_1(H_2O)_1]^-$ does not photodissociate in the spectral range studied. The $[(CO_2)_n(H_2O)_2]^-$ (n = 1, 2) species have similar spectral features with a broadband at 3340 cm^{-1}. A drastic change in the spectral features is observed for $[(CO_2)_3(H_2O)_2]^-$, where sharp bands appear at 3224, 3321, 3364, 3438, and 3572 cm^{-1}. *Ab initio* calculations are performed at the MP2/6-311++G** level to provide structural information such as optimized structures, stabilization energies, and vibrational frequencies of the $[(CO_2)_n(H_2O)_m]^-$ species. Comparison between the experimental and theoretical results reveals rather size- and composition-specific hydration manner in $[(CO_2)_n(H_2O)_m]^-$: (1) the incorporated H_2O is bonded to either CO_2^- or $C_2O_4^-$ through two equivalent OH···O hydrogen bonds to form a ring structure in $[(CO_2)_n(H_2O)_1]^-$; (2) two H_2O molecules are independently bound to the O atoms of CO_2^- in $[(CO_2)_n(H_2O)_2]^-$ (n = 1, 2); (3) a cyclic structure composed of CO_2^- and two H_2O molecules is formed in $[(CO_2)_3(H_2O)_2]^-$.

III-D Development of High-Precision Coherent Control and Its Application

Coherent control is based on manipulation of quantum phases of wave functions. It is a basic scheme of controlling a variety of quantum systems from simple atoms to nanostructures with possible applications to novel quantum technologies such as bond-selective chemistry and quantum computation. Coherent control is thus currently one of the principal subjects of various fields of science and technology such as atomic and molecular physics, solid-state physics, quantum electronics, and information science and technology. One promising strategy to carry out coherent control is to use coherent light to modulate a matter wave with its optical phase. We have so far developed a high-precision wave-packet interferometry by stabilizing the relative quantum phase of the two molecular wave packets generated by a pair of fs laser pulses on the attosecond time scale. We will apply our high-precision quantum interferometry to gas, liquid, solid, and surface systems to explore and control various quantum phenomena.

III-D-1 Space- and Time- Resolved Observation of Molecular Wave-Packet Interference on Femtosecond and Picometric Scales

KATSUKI, Hiroyuki[1]; CHIBA, Hisashi[1]; OHMORI, Kenji[1]; GIRARD, Bertrand[2]; MEIER, Christophe[2]
([1]IMS and CREST/JST; [2]Univ. Paul Sabatier)

We have developed a brand new method to observe molecular wave-packet interference in the time- and space-resolved fashion. It has been applied to the half revival of the vibrational wave packet in the iodine molecule. The observed temporal evolution of the interference has been well reproduced by the quantum mechanical calculation. We have succeeded in observing the quantum nodal structures which take place at a spatial resolution of less than 1 pm, and are created and dynamically changed on the femtosecond timescale. To our knowledge, this is for the first time that the dynamical matter-wave interferences are observed on the femtosecond time scale and picometric length scale.

III-D-2 Real-Time Observation of Phase-Controlled Molecular Wave-Packet Interference

KATSUKI, Hiroyuki[1]; HOSAKA, Kouichi[1]; CHIBA, Hisashi[1]; OHMORI, Kenji[1]; HONDA, Masahiro[2,3]; HAGIHARA, Yusuke[2,3]; FUJIWARA, Katsutoshi[3]; SATO, Yukinori[2,3]; UEDA, Kiyoshi[2,3]
([1]IMS and CREST/JST; [2]CREST/JST; [3]Tohoku Univ.)

We have controlled quantum interference of vibrational wave packets (WP's) in the iodine molecule by using a pair of phase-locked fs pulses, and the real time evolution of that interference has been observed. The real-time evolution shows a clear dependence on the inter-pulse delay $\tau_{control}$ between the locked pulses highly stabilized on attosecond time scale. We have also measured a population code, which is a population ratio among the vibrational eigenstates within a WP. The population code also shows a clear dependence on $\tau_{control}$. The ordinary frequency domain interpretation based on the spectral interference of locked pulses may be useful to elucidate population codes, but is no longer suitable for the present real-time observation. Moreover, the real-time evolution has allowed us to obtain additional phase information unable to be obtained from population codes. The combination of a population code and real-time evolution is useful to obtain both phase and amplitude information stored in a WP, which is indispensable for developing novel quantum technologies such as atom- and molecule-based information processing. All these features provides basis for opening new perspective of coherent control in a wide variety of quantum systems.

III-D-3 Development of Quantum Gate Operations with Vibrational Eigenstates of Molecules

HOSAKA, Kouichi[1]; CHIBA, Hisashi[1]; KATSUKI, Hiroyuki[1]; OHMORI, Kenji[1]; TERANISHI, Yoshiaki[2,3]; OHTSUKI, Yukiyoshi[2,3]
([1]IMS and CREST/JST; [2]CREST/JST; [3]Tohoku Univ.)

We have numerically studied quantum gate operations with the iodine molecule, based on the free temporal evolution of the vibrational wave packet and the high-precision wave-packet interferometer. The fidelities of the gate operations are found to be very high, and the proposed experimental scheme is feasible with our present experimental techniques.

III-E Quantum-State Manipulation of Molecular Motions

Molecules in gas phase undergo translational, rotational and vibrational motions in a random manner, and the total molecular system is a statistical ensemble that contains a number of molecules in many different states of motions. This research group aims to establish methods to manipulate the quantum-state distribution pertinent to molecular motions, by utilizing the coherent interaction with laser lights. Three complement methods are now being explored for manipulation of molecular motions. The first one employs creation and detection of molecular wavepackets by fs pump–probe experiments. New experimental methods for probing vibrational and/or rotational wavepackets are developed and applied to jet-cooled polyatomic systems. The second method exploits an impulsive interaction with ultrafast intense laser light to transform the initial distribution into an arbitral non-equilibrium one. We are now constructing a vacuum chamber system for this purpose. The third one utilizes an adiabatic interaction to achieve the complete population transfer, by which all the molecules are launched into states with high excitation of vibrations or rotation. We are now constructing ns laser system with sufficiently high frequency resolution to drive the adiabatic coherent interaction. Along the development of the instrument, appropriate candidates for the quantum-state adiabatic manipulation are searched. Laser spectroscopic studies are carried out to explore energy-level structure of the intermolecular vibrations in molecular clusters containing benzene.

III-E-1 Femtosecond Random-Phase Interferometry of Jet-Cooled Polyatomic Molecules

MIYAZAKI, Mitsuhiko[1]; HARUNA, Atsuyuki[2]; OHSHIMA, Yasuhiro
([1]IMS and Kyoto Univ.; [2]Kyoto Univ.)

Interferometric measurements with fs laser pulses have been extensively utilized to characterize coherent motion and decay of wavefunctions. The method, however, demands precise control of optical lengths, and it is a difficult task in particluar for shorter laser wavelength. Recently, an alternative way for fs interferometry has been demonstrated,[1),2)] in which the relative optical phase between the two laser pulses is randomly modulated while the corresponding fluctuation in fluorescence is monitored. The method termed COIN (Coherence Observation by Interference Noise) is robust to turbulence in optical lengths and thus has vast applicability. Here we have applied COIN to several polyatomic molecules to investigate wavepacket dynamics and ultrafast nonradiative processes.

In the present setup, the third harmonic with ~200 fs duration of a 1 kHz Ti:Sapphire regenerative amplifier or an output of an optical parametric oscillator was sent to a Mickelson interferometer, in which optical length of one arm was modulated by hot air stream from a blower. Two laser pulses with delay up to several hundred ps were colinearly introduced onto molecules, which were adiabatically cooled in a CW supersonic expansion. The resultant fluorescence was observed in a single shot basis, and more than 1000 laser pulses were subjected to the statistics giving the variance of fluorescence intensity at certain delay.

Rotational wavepacket dynamics has been studied by the COIN observation on the S_1–S_0 6_0^1 band of benzene. After the initial decay of coherence, weak (~5%) rotational revivals are observed in the range of 10–30 ps. The signals depend strongly on rotational temperature, and their feature is well reproduced by a model calculation with the known spectroscopic parameters. Such a sharp dependence on the rotational distribution is in pronounced contrast to the results from a related method, *i.e.*, rotational coherence spectroscopy,[3)] where gross shape of signals is not so sensitive to the temperature. The present study demonstrates the utility of COIN for monitoring the rotational distribution with high temporal resolution.

Electronic relaxation after the naphthalene S_2 excitation has also been examined by COIN. The initial coherence decays within the laser pulse duration due to the ultrafast (<< 100 fs) internal conversion from S_2 into S_1. This observation is in accord with the results from fs photoelectron spectroscopy,[4)] indicating potentiality of COIN to studies on ultrafast relaxation dynamics after photoexcitation.

References
1) O. Kinrot, *et al.*, *Phys. Rev. Lett.* **75**, 3822 (1995).
2) Ch. Warmuth, *et al.*, *J. Chem. Phys.* **112**, 5060 (2000); **114**, 9901 (2001).
3) P. M. Felker, *J. Phys. Chem.* **96**, 7844 (1992).
4) M. Schmitt, *et al.*, *J. Chem. Phys.* **114**, 1206 (2001).

III-E-2 Wavepacket Observation of Methyl Internal Rotation in *o*-Fluorotoluene

MIYAZAKI, Mitsuhiko[1]; HARUNA, Atsuyuki[2]; HASEGAWA, Hirokazu; OHSHIMA, Yasuhiro
([1]IMS and Kyoto Univ.; [2]Kyoto Univ.)

The S_1–S_0 origin region of *o*-fluorotoluene has been examined to observe wavepacket dynamics associated with internal rotation of the methyl group. In addition to COIN observation, time-resolved fluorescence depletion (TRFD) is implemented in fs time domain for the first time. The experimental arrangement for TFRD is essentially the same with COIN: total fluorescence intensity is recorded in this case as a function of delay between two fs laser pulses. Here optical cycle interference is smeared out by the random modulation in optical length, so population change induced by pump–dump process is only monitored as fluorescence depletion. The laser beam is focused at the molecular jet and fluorescence from the central part of the irradiated region is only collected to observe depletion as large as possible.

The observed TRFD and COIN spectra are shown in Figure 1, and the corresponding power spectra after

Fourier transformation are indicated in Figure 2. In the case of methyl internal rotation, the ground and the lowest excited states are coupled with *ortho* and *para* nuclear spin wavefunctions, respectively, and thus both states are populated even in adiabatically cooled jet conditions. Accordingly, TRFD spectrum is a sum of independent beats between the vibronic levels in S_1 that are optically connected with the two internal-rotation states in S_0. On the other hand, COIN spectrum exhibits all the interferences between the transitions from the two states, because it is given as the variance, *i.e.*, the average of the square of fluorescence fluctuation. The present study demonstrates the significance of the two compliment experiments in extracting the energy-level structure of the internal rotation from the time-domain observation.

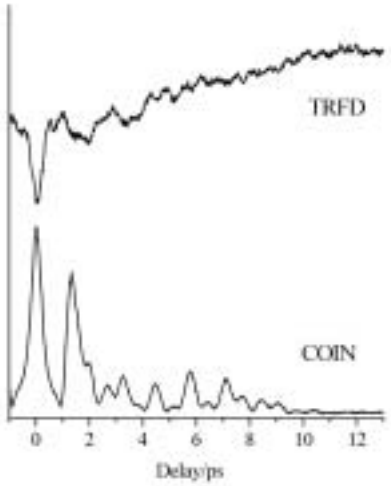

Figure 1. TRFD and COIN spectra observed by the excitation of the S_1–S_0 origin region of *o*-fluorotoluene.

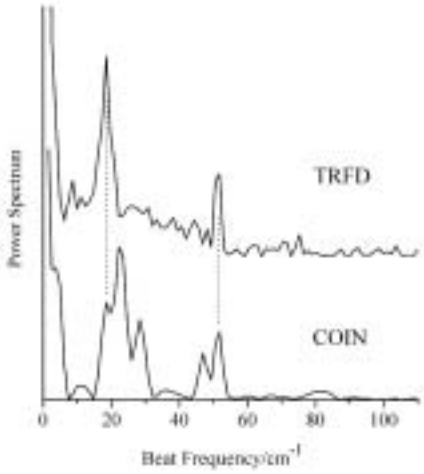

Figure 2. Power spectra obtained from the Fourier transformation of the time-domain TRFD and COIN spectra in Figure 1.

III-E-3 Construction of an Experimental Apparatus for Nonadiabatic Quantum-State Manipulation of Molecular Motions

HASEGAWA, Hirokazu; OHSHIMA, Yasuhiro

A vacuum chamber system and a data acquisition system have been designed and constructed to achieve quantum-state manipulation of molecular motions, in particular nonadiabatic molecular alignment induced by laser fields in gas phase. Molecules aligned by the interaction of intense fs laser pulses with induced electric dipole are probed through ionization. Ionization is attained by field ionization using delayed-intense fs pulses or resonance enhanced multiphoton ionization using ns laser pulses. In the former approach, dynamics of transiently aligned molecules are probed in time domain, while the change in rotational-state distribution induced by impulsive interaction with intense fs light is monitored in the latter method.

The vacuum system, composed of three differentially pumped chambers, is designed so as to be coupled with continuous or pulsed supersonic molecular beam (Figure 1). Ions produced by the interaction of laser fields with jet-cooled molecules are detected by a time-of-flight mass spectrometer. The electrode for ion extraction is designated with a small pinhole (< 1 mm), in order to ensure the detection of ions that are produced only in the region, where pump and probe laser pulses are overlapped. The integrated environment software for a data acquisition and laser control has been developed on the computer.

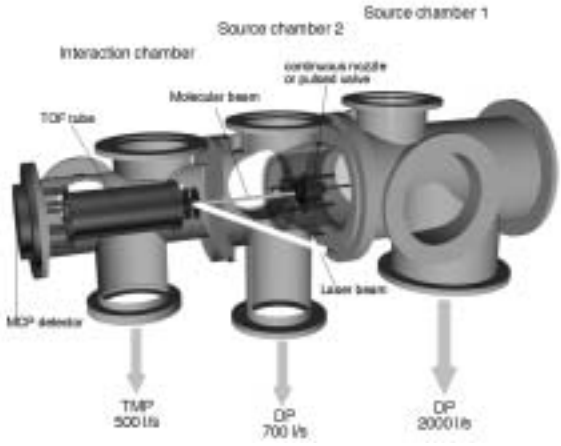

Figure 1. Vacuum chamber system for quantum-state manipulation of molecular motions.

III-E-4 Development of High-Resolution Coherent Pulsed Laser

OHSHIMA, Yasuhiro

We are constructing an all solid-state single-mode pulsed laser with Fourier-transform limited resolution ($\leq$ 0.01 cm^{-1}), for quantum-state manipulation by coherent light–matter interaction, such as stimulated Raman adiabatic passage. In the system, the output from a cw extra-cavity diode laser or a Ti:Sapphire laser injection-seeds the optical parametric amplification by BBO nonlinear crystals excited by a single-mode Nd:YAG laser. At present, we routinely achieve the output power of 20 mJ/pulse, which reaches to 20% conversion efficiency, without injection seeding. Precise adjustment of optical layout is now under way for narrow band operation by the external seeding.

III-E-5 Laser Spectroscopy of the van der Waals Vibrations of Benzene–Water

MIYAKE, Shin-ichiro[1]; MIYAZAKI, Mitsuhiko[2]; OHSHIMA, Yasuhiro
([1]Kyoto Univ.; [2]IMS and Kyoto Univ.)

Benzene-water has attracted much attention as a prototypical system containing the π hydrogen bond. Still, more experimental information should be accumulated for quantitative description of the intermolecular interaction in the complex. We have recently examine in detail the vibronic spectrum of the benzene–water 1:1 cluster pertaining to the S_1–S_0 6_0^1 transition of the benzene moiety, recorded by utilizing resonance two-photon ionization (R2PI) time-of-flight mass spectrometry. UV–UV hole-burning measurement has been performed to observe weak vibronic bands, which are buried in the R2PI excitation spectrum by background signals due to fragmentation of higher clusters. A dozen of bands associated to van der Waals (vdW) mode excitation are clearly seen in the region up to 160 cm^{-1} from the 6_0^1 transition. The vdW structure cannot be assigned as a simple combination of a few normal modes, implying a substantial anharmonic coupling between the intermolecular vibrations. In particular, the appearance of an extremely low-frequency (~8 cm^{-1}) band, similar to the case in the S_0 state, is considered to be the signature of the 3D hindered internal rotation of water in the cluster. Detailed analysis on the vdW structure is now under way with the aid of the results on isotopic variants.

III-F Photophysics and Photochemistry of Aromatic Molecules in the Condensed Phase

Excited aromatic compounds generally release energy by various pathways such as photophysical processes and photochemical reactions. Electronically excited molecules are relaxed into a stable or metastable state through radiative and/or nonradiative processes as photophysical processes. It is well known that photochemical reactions occurring from excited state are bond dissociation, cyclization, isomerization, hydrogen abstraction, electron transfer, and so on. In addition, there exist relaxation processes and their quantum yields characteristic to each compound. It is very important to investigate dynamics of photoexcited molecules.

Intermediates such as excited states and radicals, which can be generated with laser irradiation, have been detected by laser flash photolysis as described. The shorter pulse width of a light source becomes, the shorter-lived intermediates can be detected. Furthermore, the properties of intermediates would be clarified. These information should obtained photophysical and photochemical dynamics of the intermediate that are interested.

On the other hand, it becomes difficult to elucidate nonradiative processes, such as internal conversion and intersystem crossing from the excited state, by laser flash photolysis. Time-resolved photothermal techniques, however are powerful to study nonradiative processes because they can detect the released heat from excited molecules directly with high sensitivity. They should be described in detail. Combination of photoexcited and photothermal methods will give us detailed information on photophysical and photochemical dynamics of intermediates, as well as excited states.

III-F-1 Excited-State Dynamics of 4-Thiothymidine with UVA Light Irradiation

HARADA, Yosuke[1]; SUZUKI, Tadashi[1]; ICHIMURA, Teijiro[2]
([1]Tokyo Inst. Tech.; [2]IMS and Tokyo Inst. Tech.)

Thionucleobases and thionucleosides have received renewed attention because of their distinct property, namely, high sensitivity to UVA light (320–400 nm) in which region normal DNA constituents are transparent. 4-Thiothymidine (4-TT), an analogue of the naturally occurring nucleoside thymidine, has strong absorption in the UVA region. Recently it was reported that 4-TT can be readily incorporated into cellular DNA and that low doses of UVA light can easily inflict lethal damage on the DNA containing 4-TT, causing cell death. The synergistic use of 4-TT and UVA light offers a novel approach to cancer treatment. Apparently, electronically excited state of 4-TT is at the initial and crucial stage of the UVA-induced cell killing, and thus photophysical and photochemical studies of 4-TT would be of great significance.

We have measured transient absorption spectrum of 4-TT in deaerated acetonitrile with the nanosecond 355 nm laser. Immediately after the laser shot, an intense bleaching at 335 nm and a broad absorption band at 380–600 nm (Abs. Max. 530 nm) were observed. The bleaching is ascribed to the depletion of the ground state molecules while the absorption band is assigned to the absorption of the lowest excited triplet (T_1) state of 4-TT (T–T absorption). The T–T absorption decayed with the rate constantof 1×10^6 s^{-1}. In triplet quenching experiments by KI, the absorption intensity of the photoproducts decreased correspondingly to shortening of triplet lifetime of 4-TT. Our experimental results suggest that photochemical process would take place *via* the T_1 state of 4-TT and other several intermediate states. A good understanding of the photophysics and photochemistry of 4-TT could offer valuable insights to the mechanisms by which cancer cells are killed.

III-F-2 Photochemical Reaction Dynamics of *o*-Quinones

HARADA, Yosuke[1]; WATANABE, Sadayuki[1]; SUZUKI, Tadashi[1]; ICHIMURA, Teijiro[2]
([1]Tokyo Inst. Tech.; [2]IMS and Tokyo Inst. Tech.)

[*J. Photochem. Photobiol., A* **170**, 161–167 (2005)]

Photoreaction dynamics of 9,10-phenanthrenequinone (PQ) and 1,2-naphthoquinone (NQ) in solution has been studied by laser flash photolysis technique. The real-time transient absorption measurements found out; (1) by excitation at 355 nm in the presence of alcohol, absorption band characteristic to the quinone ketyl radical emerged as the triplet–triplet (T–T) absorption of the quinone submerged, (2) the rise of the absorption of the ketyl radical consisted of two components; the fast and slow ones, where the fast one had the rise rate constant corresponding to the decay rate of triplet quinone, while the slow one rose up much slowly. The experimental fact clearly revealed that the slow reaction should give rise to formation of the ketyl radical following the hydrogen abstraction of triplet PQ and NQ from alcohol, and should be attributed to the hydrogen atom transfer between the parent quinone in the ground state and counter α-hydroxyalkyl radical produced from alcoholic molecule. In this study, we carried out the real-time measurement and clarified the reaction mechanism between the α-hydroxyalkyl radicals and the ground state quinones.

Triplet PQ and NQ show remarkable high reactivity with benzene. The notable reactivity would result from their characteristic molecular conformation; namely, the existence of two adjacent carbonyl groups would cause the stabilized conformation in the transition state through doubly hydrogen bonding with the hydrogen donor.

III-F-3 Evidence of Phenoxymethyl Radical Formation in Laser Photolysis of Anisole in Solution

ANDO, Mayaka[1]; YOSHIIKE, Shigeru[1]; SUZUKI, Tadashi[1]; ICHIMURA, Teijiro[2]; OKUTSU, Tetsuo[3]; UEDA, Minoru[3]; HORIUCHI, Hiroaki[3]; HIRATSUKA, Hiroshi[3]; KAWAI, Akio[1]; SHIBUYA, Kazuhiko[1]
([1]Tokyo Inst. Tech.; [2]IMS and Tokyo Inst. Tech.; [3]Gunma Univ.)

[*J. Photochem. Photobiol., A* **174**, 194–198 (2005)]

Transient absorption spectrum of anisole in acetonitrile was observed by a 248-nm laser photolysis. In addition to the structured band observed at 400 nm, which was assigned to phenoxyl radical, a broad absorption band appeared at around 440 nm. The lifetime of the unknown species was not affected by oxygen. By means of acetone photosensitization reaction, photolysis of 1,2-diphenoxyethane, and ESR measurements, the species was assigned to phenoxymethyl radical, produced with two-photon absorption through the S_1 state of anisole to form anisole cation and consecutive deprotonation of the cation.

III-F-4 Production and Excited State Dynamics of the Photorearranged Isomer of Benzyl Chloride and Its Methyl Derivatives Studied by Stepwise Two-Color Laser Excitation Techniques

NAGANO, Mika[1]; SUZUKI, Tadashi[1]; ICHIMURA, Teijiro[2]; OKUTSU, Tetsuo[3]; HIRATSUKA, Hiroshi[3]; KAWAUCHI, Susumu[1]
([1]Tokyo Inst. Tech.; [2]IMS and Tokyo Inst. Tech.; [3]Gunma Univ.)

[*J. Phys. Chem. A* **109**, 5825–5831 (2005)]

Production and photoexcited dynamics of reaction intermediates with photolyses of benzyl chloride (BzCl) and methyl-substituted benzyl chlorides (MeBzCls) were studied by using stepwise two-color laser excitation transient absorption (TC-TA) and two-color laser excitation time-resolved thermal lensing (TC-TRTL) measurements. With photoexcitation of BzCl the formation of transient photo-rearranged isomer was suggested in the previous paper.[1)] Such an isomer formation for MeBzCls was also observed in a 248 nm excitation. It was found that further photoexcitation of the isomers with the 308 nm light caused photodissociation to yield the corresponding benzyl radicals. The reaction quantum yield and the molar absorptivity of the photorearranged isomer of BzCl were estimated. The heat of reaction for the photodissociation of the isomer was successfully determined with the TC-TRTL measurement. These experimental results were consistent with MO calculations.

Reference

1) H. Hiratsuka, T. Okamoto, S. Kuroda, T. Okutsu, H. Maeoka, M. Taguchi and T. Yoshinaga, *Res. Chem. Intermed.* **27**, 137–153 (2001).

III-G Spectroscopy and Excited State Dynamics of Jet-Cooled Aromatic Molecules

The phenomena of energy relaxation in isolated molecules have been central in chemical kinetics over many decades. An extensive subject has been followed by the application of supersonic jet techniques, which enabled the study of well isolated ultra-cold molecules. The jet-cooled molecules are isolated in gas phase, thus, the experiments are not subjected to interactions between molecules and solvents or to vibrational relaxation in condensed phases.

The large transition energy is reserved in optically electronic exited molecules where the idea of temperature for molecular internal energy is replaced by the excess energy, by which photodissociation is induced. Investigation of nonradiative electronic relaxation processes, *i.e.* internal conversion (IC) or intersystem crossing (ISC) between two electronic states of the same or different electron spin multiplicity of photoexcited molecules, respectively, has long been interest of the photochemical dynamics because of the important role of these processes in photochemical reaction system.

A triplet state serves as an important intermediate in nonradiative processes of excited molecules. The dynamics of the triplet state generation, *i.e.* ISC, plays an important role in photochemical processes. For instance, chlorinated benzene derivatives in the first excited singlet (S_1) state have small values (10^{-2}) of the fluorescence quantum yields, suggesting that the ISC process to excited triplet states takes place due to the large spin-orbit coupling induced by the heavy Cl atom effect. The excited triplet state molecules undergo the C–Cl dissociation whose quantum yield is almost unity. Accordingly, the investigation of the ISC process assists to understand the photochemical reactions.

The substituent of the CH_3 or OCH_3 group on the benzene ring should play an important role in their photoexcited states. When these molecules are excited to the singlet excited state, internal rotational bands of these groups are observed for lower frequency regions than 200 cm^{-1} in the LIF excitation spectra. Measurements of these internal band intensities and their fluorescence lifetimes should give information on the relaxation dynamics of these molecules.

III-G-1 Spectroscopy and Relaxation Dynamics of Photoexcited Anisole and Anisole-d_3 Molecules in a Supersonic Jet

MATSUMOTO, Ryu[1]; SAKEDA, Kosaku[1]; MATSUSHITA, Yoshihisa[1]; SUZUKI, Tadashi[1]; ICHIMURA, Teijiro[2]
([1]Tokyo Inst. Tech.; [2]IMS and Tokyo Inst. Tech.)

[*J. Mol. Struct.* **735-736**, 153–167 (2005)]

The vibronic structures of the S_1–S_0 electronic transitions of jet-cooled anisole and anisole-d_3 molecules have been investigated in detail using the laser induced fluorescence and single vibrational level dispersed fluorescence (DF) spectroscopy. Normal mode frequencies of the ground and excited states including the methyl and methoxy internal rotations were determined by analyses of dispersed fluorescence spectra and molecular orbital calculations. Strong vibrational mixing in the S_1 state was observed in several DF spectra. Duschinsky rotation between 6a and 6b modes prominently appeared for both molecules and it was found that methyl deuteration depressed the second-order vibronic coupling of these modes. Another explicit Duschinsky rotation was found in 10b and 16a modes of both molecules. However, in the case of the deuterated molecule the mixing cannot be explained by only Duschinsky rotation. A Fermi resonance due to level proximity should be involved in the mixing scheme. Vibronic bands in the higher frequency regions exhibit broadened and structureless fluorescence due to intramolecular vibrational energy redistribution (IVR). The onset of the IVR process inferred from the DF spectra was found to be increased by methyl deuteration on the contrary to general propensity rule. The deuteration effect is characteristic of anisole molecules and indicates considerable decrease in the interaction with the dark bath modes. Fluorescence lifetime measurements suggest the enhancement of intersystem crossing in the levels with out-of-plane vibrational components. The observed broadening of DF spectra corresponded to nonradiative decay rates from levels with the in-plane vibrational modes. This suggests that the energy flow into out-of-plane bath modes through the IVR process should dominate nonradiative rates on initially excited in-plane vibrational levels. Our analysis clarified that the out-of-plane vibrations accompanying the methoxy motion make large contribution to the relaxation dynamics.

III-G-2 Internal Rotational Motion of the Chloromethyl Group of the Jet-Cooled Benzyl Chloride Molecule

MATSUMOTO, Ryu[1]; SUZUKI, Tadashi[1]; ICHIMURA, Teijiro[2]
([1]Tokyo Inst. Tech.; [2]IMS and Tokyo Inst. Tech.)

[*J. Phys. Chem. A* **109**, 3331–3336 (2005)]

The mass-resolved resonance enhanced two-photon ionization spectra of jet-cooled benzyl chloride were measured. Some low-frequency vibronic bands around the S_1–S_0 origin band were assigned to transitions of the internal rotational mode of the chloromethyl group. The internal rotational motion was analyzed by using the one-dimensional free rotor approximation. The conformation in the S_1 state was found to be that in which the C–Cl bond lies in orthogonal to the benzene plane. For the species with *m*/*e* 126, the transition energy of the internal rotational bands corresponded well to the potential energy values of V_2 = 1900 cm^{-1} and V_4 = 30 cm^{-1} in the S_1 state and the reduced rotational constant B values 0.50 and 0.47 cm^{-1} in the S_0 and S_1 states, respectively. The B values obtained for the chlorine isotopomer (*m*/*e* 128) were slightly different. The S_1 potential barrier height was found to be about 3 times larger than that for the S_0 state. Molecular orbital calculations suggest that the difference between energies of the HOMO and LUMO with respect to the rotation of the chloromethyl group correspond approximately to the potential energy curve obtained for the S_1 state.

III-G-3 Molecular Structure and Excited State Dynamics of Jet-Cooled *o*-, *m*- and *p*-Fluoroanisole

ISOZAKI, Tasuku[1]; SAKEDA, Kosaku[1]; SUZUKI, Tadashi[1]; ICHIMURA, Teijiro[2]
([1]Tokyo Inst. Tech.; [2]IMS and Tokyo Inst. Tech.)

Intramolecular isomerism plays a significant role in biologically relevant molecular systems such as the folding of proteins and molecular machines. In understanding the function of the complicated large biological molecules, it is important to know the conformational properties and excited state dynamics of their local units. In this point of view, the molecular structure and relaxation dynamics of anisole derivatives were studied. It is known that *meta*-substituted anisole has two stable *planar* conformers (*i.e. cis* and *trans*), which are raised from the orientation of the methoxy group with respect to the substituent. Our aim is to clarify fluorination effect against anisole on the electronic transitions, conformational structure, vibronic structure and relaxation dynamics of *o*-, *m*- and *p*-fluoroanisole (FA).

We measured the laser-induced fluorescence (LIF) excitation and single vibronic level (SVL) dispersed fluorescence spectra of jet-cooled *o*-, *m*- and *p*-FA. The SVL dispersed fluorescence spectra were also measured by pumping each vibronic band. The observed bands were assigned with the aid of the quantum chemical calculations. The SVL dispersed fluorescence spectra indicated that the vibrational band mixing should take place in the S_1 state, and the IVR process becomes more dominant with the higher excess energy. The vibrational band mixing and IVR process are characteristic for each isomer.

III-G-4 Evidence for a Non-Planar Conformer and Conformational Isomerization of *o*-Fluoroanisole in a Low-Temperature Ar Matrix

ISOZAKI, Tasuku[1]; SAKEDA, Kosaku[1]; SUZUKI, Tadashi[1]; ICHIMURA, Teijiro[2]; TSUJI, Kazuhide[1]; SHIBUYA, Kazuhiko[1]

([1]Tokyo Inst. Tech.; [2]IMS and Tokyo Inst. Tech.)

[*Chem. Phys. Lett.* **409**, 93–97 (2005)]

FT-IR spectra of *o*-fluoroanisole were measured in a low-temperature Ar matrix with and without UV irradiation. The observed bands, without irradiation, were assigned to the *trans* conformer with the aid of the quantum chemical calculations at the B3LYP/cc-pVTZ level. By comparing the IR spectrum, after irradiation, with the calculated spectra, the formation of a *non-planar* conformer was established. The *non-planar* conformer gradually decayed by a unimolecular process under dark conditions at 16 K, while the *trans* conformer increased. The back-reaction rate was estimated, and the reaction dynamics between the *trans* and *non-planar* conformers was discussed.

III-G-5 Molecular Structure and Puckering Vibration of 1-Aminoindan in a Supersonic Jet

IGA, Hiroshi[1]; ISOZAKI, Tasuku[1]; SUZUKI, Tadashi[1]; ICHIMURA, Teijiro[2]
([1]Tokyo Inst. Tech.; [2]IMS and Tokyo Inst. Tech.)

The laser-induced fluorescence (LIF) and single vibronic level dispersed fluorescence spectra of 1-aminoindan (1-AI) were measured in a supersonic jet. Two prominent intense bands observed at 36934 and 37062 cm^{-1} in the LIF spectrum were assigned to the 0^0 bands of rotational isomers resulting from the orientation of the amino group. The low-frequency puckering vibration was compared with indan. The puckering frequency and transition intensity of 1-AI are the same as indan in the S_0 state and not in the S_1 state. The quantum chemical calculations suggest six possible isomers, however, only two stable rotational isomers were observed in the spectra. The intramolecular N–H$\cdot\cdot\pi$ hydrogen bond should play an important role in the stabilization of the rotational isomers.

III-H Photochemical Reactions in Microreactors

Many chemical synthesis has been so far conducted by temperature controlled chemical reactions using specific catalyst. Utilization of characteristic catalyst, however, is restricted to some enantioselective synthetic reactions. Light is a powerful tool to excite molecules into electronically excited states selectively to give rise to specific reaction channel. Our proposal is application of laser light to elucidate the mechanism of photo-induced chemical reactions taken place in micro-region reaction vessel. Laser light has a couple of advantages to investigate the reaction mechanism, such as high power, time-resolved analysis, and polarization character (linear or circular dichroism), that is specifically related to characteristic properties of the enantiomer. Another feature of the laser light is a small beam divergence, of which diameter still can be focused into much smaller area such as micrometer region. Taking into account of these considerations, we have set up the laser photochemical synthesis system and photocatalytic reaction system with immobilized titanium dioxide. Both the laser irradiation system and the product analysis section can be processed on the same site of the microreactor. The products generated by the laser irradiation can be analyzed at the downstream site of the reactor using a second laser irradiation. If the product emits the detectable fluorescence, the LIF measurement can be applicable. In case of non-emitting substance an opto-acoustic and/or photothermal spectroscopy, or Raman spectroscopy should be employed. We have investigated enantioselective reaction of cyclooctene derivatives as a model system, and photocatalytic degradation of endocrine disruptors with immobilized titanium dioxide.

III-H-1 Application of Microfabricated Reactors for Asymmetric Photoreaction

ICHIMURA, Teijiro[1]; KUMADA, Shinji[2]; WAKABAYASHI, Kazuhito[2]; SAKEDA, Kosaku[2]; MATSUSHITA, Yoshihisa[2]; SUZUKI, Tadashi[2]
([1]IMS and Tokyo Inst. Tech.; [2]Tokyo Inst. Tech.)

[*2nd International Conference on Green and Sustainable Chemistry* (2005)]

We reinvestigated the asymmetric photoreaction of enantiodifferentiating Z-*E* photoisomerization of cyclooctene sensitized by aromatic esters in a microreactor. Effects of residence time, temperature, and laser power on the photoreaction were investigated. The results indicate that high ee value was obtained within the short residence time. In contrast, the longer residence time was required to achieve higher *E*/Z ratio. The higher laser power and/or reputation rate becomes, the quicker the *E*/Z ratio should reach to the highest value. The ee value was quite sensitive to the temperature. The reaction mechanism will be discussed in terms of the conformational structure of excimer.

III-H-2 Photocatalytic Reaction in Microfabricated Reactors

MATSUSHITA, Yoshihisa[1]; KUMADA, Shinji[1]; WAKABAYASHI, Kazuhito[1]; SAKEDA, Kosaku[1]; ICHIMURA, Teijiro[2]
([1]Tokyo Inst. Tech.; [2]IMS and Tokyo Inst. Tech.)

[*The Third International Workshop on Micro Chemical Plants* (2005)]

Photocatalytic reaction in microspace was investigated by using a microreactor with immobilized tita-

nium dioxide. Since a photocatalytic reaction takes place on an irradiated titanium dioxide surface, a microfabricated reactor which has a large surface-to-volume ratio must prove its advantages on the reaction.

Photodegradation of endocrine disruptors was examined as a model reaction. The microreactors made of quartz with a cross-section of 0.5 mm width and 0.1–0.5 mm depth were coated with a photocatalytic titanium dioxide layer of approximately 1 micron thickness. Aqueous solutions of 3-chlorophenol, monochlorobenzene, bisphenol A, and *N*,*N*-dimethylformamide were introduced to the microreactor with a syringe pump then irradiated with a UV light source. The following light sources were employed for the excitation of photocatalytic titanium dioxide: XeCl (308 nm) excimer laser, YAG (355 nm) laser and OPO laser (300–400 nm) excited with the YAG laser, and UV-emitting diodes (UV-LED, 365, 375 and 385 nm).

The variation profiles of the concentration of endocrine disruptors as a function of irradiation time were examined. Degradation increased with increasing the residence time and reaches 30% for 3-chlorophenol and 13% for bisphenol A at a irradiation time of 5 seconds in the case of 385 nm UV-LED excitation with a microreactor of 0.1 mm depth. Higher degradation was obtained for lower concentrations of endocrine disruptors and smaller thickness of microspace. Degradation kinetics and photonic efficiencies dependent on the nature of the light source are further discussed.

Feasibility of phtotocatalytic reaction in microreactors was thus proven and optimization of excitation wavelength and photon density, design of the microreactor, and flow rate and irradiation time are under progress for the establishment of the photocatalytic microreaction system.

III-I In-Situ Observation of Surface Reactions by Variable Temperature Scanning Tunneling Microscopy

Chemical reactions at a well-defined single crystal surface has been intensively investigated as a prototype for heterogeneous catalytic reaction, electrochemical reaction and corrosion. The surface chemical reactions are heterogeneous in nature reflecting the structural and electronic imperfections relevant to steps, vacancies and impurities. In addition, the surface reactions are significantly influenced by the presence of reactants and products which often form ordered arrays. Therefore, in order to get better understanding of the surface reactions, it is vital to unravel the nature of these local properties which are closely linked to catalytic activity. The advent of scanning tunneling microscopy (STM) has enabled us to tackle the challenge with the ability to image the surface reactions in both real-time and real-space with atomic resolution. We investigate the reactivity of novel one-dimensional (1D) –Ag–O–Ag–O– compounds formed upon the dissociative adsorption of oxygen molecule on Ag(110) using variable temperature STM (VT-STM). The 1D compounds are arranged periodically to form (n×1) (n = 2–7) reconstructed structures. In addition, the 1D compounds show structural fluctuation in low O coverage regime reflecting the low dimensionality. These characteristics make them promising as a model system to explore physical and chemical properties of nano-structured materials.

III-I-1 In-Situ Observation of CO Oxidation on Ag(110)(2x1)-O by Scanning Tunneling Microscopy: Structural Fluctuation and Catalytic Activity

NAKAGOE, Osamu[1]; WATANABE, Kazuya[2]; TAKAGI, Noriaki[3]; MATSUMOTO, Yoshiyasu[2]
([1]Hokkaido Univ.; [2]IMS and SOKENDAI; [3]IMS and Univ. Tokyo)

[*J. Phys. Chem. B* **109**, 14536–14543 (2005)]

On the added-row reconstructed Ag(110)(n×1)-O surfaces where one-dimensional –Ag–O–Ag–O– chains arrange periodically, the clean-off reaction of O adatoms by CO was investigated using variable temperature scanning tunneling microscopy (VT-STM). Based on the *in-situ* STM observations of the surface structure variation in the course of the reaction at various temperatures, we found that the reaction kinetics are significantly affected by the structural transition of AgO chains from a solid straight line configuration to dynamically fluctuating configurations. Below 230 K where the chains are straight, the reaction takes place only at the end of the chains, so that the reaction progresses in the zeroth order kinetics with the reaction front propagating along the chain. The temperature dependence of the reaction rates yields the activation barrier of 41 kJ/mol and the pre-exponential factor of 1.7×10^3 $cm^{-2}s^{-1}$. At room temperature, the reaction rate is drastically accelerated when almost half of O adatoms are eliminated and the chains start fluctuating. The dynamic formation of active sites equivalent to the end of chains upon the chain fluctuation results in the nonlinear increase of the reaction rate.

III-I-2 Propagation of Reaction Front in the Disproportionate Reaction of H_2O on Ag(110)(5x1)-O Surface: Role of Hydrogen Bonding Interaction

TAKAGI, Noriaki[1]; NAKAGOE, Osamu[2]; WATANABE, Kazuya[3]; MATSUMOTO, Yoshiyasu[3]
([1]IMS and Univ. Tokyo; [2]Hokkaido Univ.; [3]IMS and SOKENDAI)

[*J. Phys. Chem. B* **109**, 14536–14543 (2005)]

The structural evolution in the course of the disproportionation of H_2O with O adatoms in the added-row reconstructed Ag(110)-O surfaces was investigated by variable temperature scanning tunneling microscopy. Initially, the reaction takes place only at the ends of the added-rows, and then, after the induction period, the reaction progresses explosively with the reaction front propagating at the rate of 1 nm/s. The strong nonlinearity can be explained by the autocatalytic reaction model where clustering of H_2O by the hydration of OH makes both H_2O coverage and reactivity of H_2O sufficiently high that a new reaction pathway opens to drive the reaction front.